Role of spectator decay and final-state mixing in resonant photoemission of La metal

S. L. Molodtsov*

Institut für Oberflächen- und Mikrostrukturphysik, Technische Universität Dresden, D-01062 Dresden, Germany

Yu. Kucherenko

Institute of Metal Physics, National Academy of Sciences of Ukraine, 252142 Kiev, Ukraine

J. J. Hinarejos[†] and S. Danzenbächer

Institut für Oberflächen- und Mikrostrukturphysik, Technische Universität Dresden, D-01062 Dresden, Germany

V. D. P. Servedio and M. Richter

Group for Theoretical Solid State Physics, Institut für Festkörper- und Werkstofforschung, P.O. Box 270016, D-01171 Dresden, Germany

C. Laubschat

Institut für Oberflächen- und Mikrostrukturphysik, Technische Universität Dresden, D-01062 Dresden, Germany

It is shown that the La $5p$ photoemission (PE) spectra consist of a superposition of two final states reflecting predominantly $5p^54f^0$ and $5p^54f^1$ character. In contrast to La $3d$ spectra, the $4f^1$-derived component appears at the high-binding-energy side of the $4f^0$-derived emission due to a weaker interaction between the photohole and the $4f$ electron. This splitting into two components is crucial for the quantitative understanding of the resonant behavior of the $5p$ states at the $4d \rightarrow 4f$ excitation threshold. In addition to the participator decay channel usually considered for the description of the resonant PE, a spectator decay channel must be taken into account that leads particularly to an enhancement of the $4f^1$ originating emission. The contributions of the spectator transitions are particularly important in the range of the so-called preresonances, e.g., at the $^3P_1$ and $^3D_1$ excitation thresholds. [S0163-1829(99)03647-4]

I. INTRODUCTION

During the last twenty years resonant photoemission (PE) has been developed to a powerful tool for the investigation of the electronic structure of solids.[1] This method takes advantage of a resonant variation of the photoionization cross section that takes place if the photon energy is tuned across certain core-level excitation thresholds. The underlying mechanism is frequently described as a Fano resonance caused by a coupling of the direct PE channel with another, indirect channel that is realized by a core excitation into a discrete intermediate state and subsequent autoionization. Closely above the excitation threshold, a constructive interference of these channels leads to an increase of the photoionization cross section, while somewhat below the threshold a destructive interference results in a strong suppression of electron emission.

This phenomenon is due to the existence of localized intermediate states. Thus, the resonant PE is particularly applicable to transition metals,[2] rare earths (RE's),[3–7] and actinides.[8] Best studied is the $4d \rightarrow 4f$ resonance of RE's, where a $4d$ electron is excited from a $4d^{10}4f^n(5d6s)^x$ initial state to form a $4d^94f^{n+1}(5d6s)^x$ intermediate state. Autoionization leads to emission of a $4f$, $5p$, $5s$ core or a $(5d6s)$ valence electron.[6,9] For the decay mechanisms, usually only participator processes are considered, where at least one $4f$ electron (two in case of $4f$ emission) is involved.[10–12] The latter is justified, because the participator channels represent Coster-Kronig or even super-Coster-Kronig processes

that are usually characterized by higher transition probabilities than those of other autoionization events. Considering the multiplet structures in the intermediate and final states, however, the participator channels in certain cases could be suppressed by selection rules, and spectator processes become important.

In the present paper we discuss possible consequences of the above consideration for the simplest model system available, namely La metal. As a free atom, La reveals a trivalent $[\text{Xe}]4f^0(5d6s)^3$ configuration. In the condensed phase, fd hybridization may result in configuration mixing. However, since the $4f^1$ configuration lies about 5 eV above the Fermi energy (E_F),[13] the $4f^1$ admixtures to the ground state are negligibly small and do not affect the ground-state properties. Upon core-level PE, the $4f^1$ configuration becomes energetically lowered with respect to the $4f^0$ state due to interaction with the photohole and configuration mixing increases. As a consequence, two different PE final states become accessible, labeled ϕ^0 and ϕ^1. Both contain $4f^0$ and $4f^1$ admixtures, but in the ϕ^0 final state the $4f^0$ component is dominant, whereas for the ϕ^1 state the situation is reversed. This scenario is well known from the La $3d$ PE studies, where the ϕ^1 signal appears as a shoulder at the low-binding-energy (BE) side of the ϕ^0 emission.[14] As we will show in the present contribution, a similar situation is also encountered for the $5p$ core-level PE spectra. In contrast to the $3d$ case, however, the ϕ^1 state is found at the high-BE side of the ϕ^0 emission due to a weaker interaction between photohole and $4f$ electron. At the $4d \rightarrow 4f$ excitation thresh-

old, participator decays of the $4d^9 4f^1$ intermediate states predominantly contribute to ϕ^0 final states and are responsible for the giant enhancement of the $5p$ emission intensity at the $^1P_1$ resonance. Spectator processes, on the other hand, mainly result in ϕ^1 final states and significantly influence the emission behavior in the range of the so-called preresonances $^3P_1$ and $^3D_1$, where transition rates of participator processes are strongly reduced.

II. EXPERIMENTAL DETAILS

Films of La metal were thermally evaporated from a Knudsen cell onto a polycrystalline Cu substrate. The evaporation rate (4 Å /min) and the thickness of the deposited films (about 200 Å) were calibrated by means of quartz microbalances. Possible contaminations were controlled by monitoring the PE responses in the energy regions of the O $1s$ and C $1s$ core levels as well as by valence-band PE measurements. The base pressure during the measurements was always lower than 1×10^{-10} mbar. PE and x-ray absorption spectroscopy (XAS) experiments in the region of the La $4d$ $\rightarrow 4f$ excitation threshold were performed at the SX700/II beamline of the Berliner Elektronenspeicherring für Synchrotronstrahlung BESSY I using a rotatable hemispherical electron energy analyzer (ARIES-VSW). All PE spectra were taken at normal emission geometry with an overall system resolution of ≈ 150 meV (full width at half maximum, FWHM). XAS measurements were performed in a partial electron yield mode by acquisition of 2-eV kinetic energy electrons.

III. FINAL-STATE MIXING

Many-body effects in PE core-level spectra of RE systems have successfully been described in the framework of a single-impurity Anderson model.[15] For La, a rather simple formulation presented by Imer and Wuilloud[16] may be applied: Only two basis states, $4f^0$ and $4f^1$, are considered at binding energies of 0 and ε, respectively. A hybridization parameter Δ describes the electron hopping between valence band and f orbitals that leads to configurationally mixed states ϕ^0 and ϕ^1. Upon creation of a core hole, the $4f^1$ basis state becomes energetically lowered by the Coulomb interaction, U_{fc} (see right panel in Fig. 1). The core-level PE spectrum then consists of two components, a dominant signal at energy E_0 originating from the ϕ^0 state and a ϕ^1 contribution at energy

$$E_1 = E_0 + (\varepsilon - U_{fc}) \left(1 + \frac{4\Delta^2}{(\varepsilon - U_{fc})^2} \right)^{1/2}. \quad (1)$$

The magnitude of U_{fc} depends on the charge distribution of the core hole with respect to the $4f$ orbital: For a $3d$ hole, the charge density lies mainly inside the $4f$ shell (inset in Fig. 1), and the effective Coulomb interaction estimated from density-functional theory (DFT) amounts to $U_{fc} \approx 9.5$ eV.[17] For a $5p$ hole, on the other hand, a large fraction of the charge density lies outside the $4f$ shell, and a value $U_{fc} \approx 2.5$ eV is obtained. Taking $\varepsilon = 5.2$ eV from inverse PE data[13] we arrive at the result [Eq. (1)] that independent of the special choice of Δ the ϕ^1 component is found on the
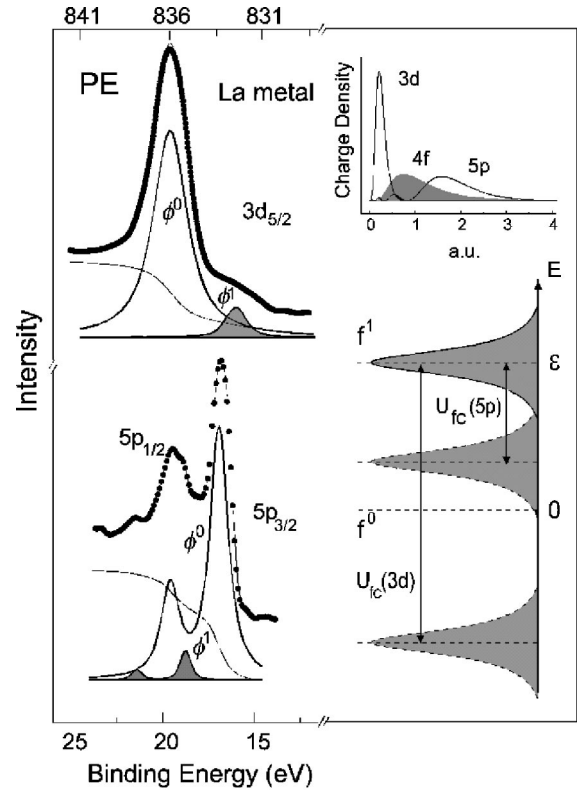

FIG. 1. *Left panel*: $5p$ and $3d_{5/2}$ PE spectra (lines through experimental points) taken at $\hbar\omega = 100$ eV and 1486.6 eV (Ref. 14), respectively. Results of least-squares fit analyses applying a simple formulation of single-impurity Anderson model (Ref. 16) are shown underneath the experimental curves. *Right panel*: Lowering of the $4f^1$ state due to the Coulomb interaction U_{fc} with a $3d$ and a $5p$ core hole (dashed curves). The solid curve denotes the $4f^1$ position if no hole is present. *Inset*: Radial distributions of charge densities of the $3d$, $4f$, and $5p$ electrons.

low-BE side of the ϕ^0 component for $3d$ emission, while it is expected on the high-BE side for $5p$ emission.

Nonresonant PE spectra of the La $3d_{5/2}$ and La $5p$ core levels are shown in the left panel of Fig. 1. The La $3d_{5/2}$ spectrum reveals the well-known splitting into ϕ^0 and ϕ^1 final states.[14] The La $5p$ spectrum is characterized by a dominant doublet structure that stems from the spin-orbit-split $5p_{1/2}(\phi^0)$ and $5p_{3/2}(\phi^0)$ components. Closer inspection, however, reveals a second doublet component that is shifted with respect to the main lines by about 2.1 eV toward higher BE and may be attributed to final states $5p^5(\phi^1)$ with predominantly $5p^5 4f^1$ character. Both the $3d$ and the $5p$ PE spectra may be described consistently within a least-squares fit analysis using $\varepsilon = 5.2$ eV and $\Delta = 0.7$ eV. The respective U_{fc} obtained from DFT (see above) were taken as starting fit parameters. Then, energy positions and relative intensities were calculated within the Imer-Wuilloud approach.[16] For the line shapes, Lorentzians convoluted with Gaussians to account for the finite experimental resolution were assumed. They were superimposed by an integral background approximating inelastic electron scattering. Surface effects[18] were neglected for the sake of simplicity. In the course of the fitting we arrive at $U_{fc} = 8.6$ eV and 3.6 eV for the $3d$ and $5p$ holes, respectively, in fair agreement with the DFT values. For the final states with a $5p$ hole this results in an
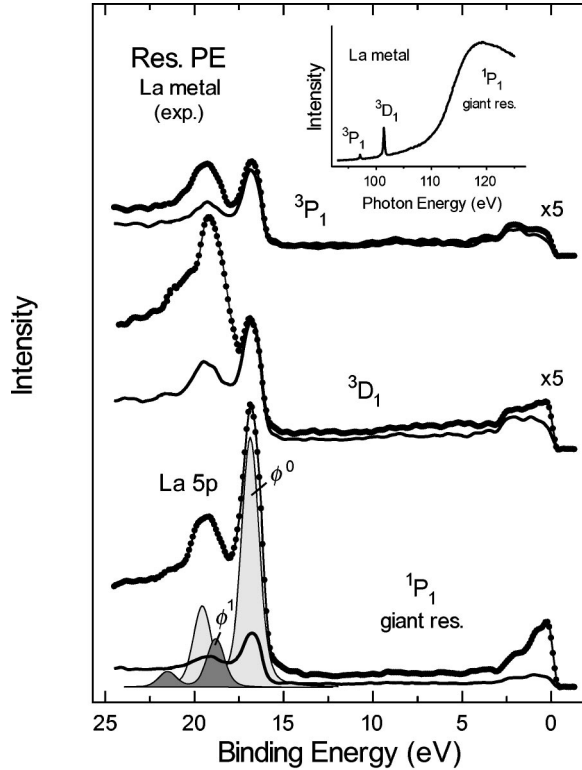
FIG. 2. On-resonance PE spectra (lines through experimental points) taken upon excitation into the $^3P_1$, $^3D_1$, and $^1P_1$ intermediate states with $\hbar\omega = 97$ eV, 101 eV, and 117 eV, respectively. Corresponding off-resonance spectra (thick lines) were taken at $\hbar\omega = 96.5$ eV, 100.5 eV, and 112 eV. All spectra are normalized to photon flux. Results of a least-squares fit analysis are shown underneath the La $5p$ spectrum taken upon excitation into the $^1P_1$ resonance. Inset shows a XAS spectrum recorded at the $4d \rightarrow 4f$ excitation threshold.

energy separation of the components $\Delta E = E_1 - E_0 = 2.1$ eV. The related mixed final states $|\phi^i\rangle$ are expressed by linear combinations of the atomic configurations $|f^0\rangle = |5p^5 4f^0 5d^x\rangle$ and $|f^1\rangle = |5p^5 4f^1 5d^{x-1}\rangle$,

$$|\phi^i\rangle = c_{i0}|f^0\rangle + c_{i1}|f^1\rangle, \quad i = 0,1 \qquad (2)$$

with mixing coefficients $c_{00} = c_{11} = 0.94$ and $c_{10} = -c_{01} = 0.35$.

IV. RESONANT PHOTOEMISSION

A. Qualitative considerations

At the La $4d \rightarrow 4f$ excitation threshold, three different intermediate states can be populated[19] as it can be seen from the XAS spectrum shown in the inset of Fig. 2: The main peak of the XAS spectrum at 117-eV photon energy corresponds to a $^1P_1$ state and is the only one that can be reached by a dipole transition from the $^1S_0$ ground state of La^{3+}, if LS coupling is assumed. Considering intermediate coupling, also $^3P_1$ and $^3D_1$ states may be populated, leading to the preresonances at 97 eV and 101 eV photon energies, respectively. The excitation threshold for transitions into continuum states is given by the La $4d$ binding energy of 102 eV.

As it is usual in literature[10,19,20] we use the notations for multiplet components of free La^{3+} ions, although the valence electrons are considered to be involved into the decay processes. Note that due to the intermediate coupling the $^3P_1$, $^3D_1$, and $^1P_1$ states differ from pure LS states. Solid-state hybridization effects in the intermediate states are neglected, because they are small as compared to multiplet splitting as it is evident from the good agreement of the XAS data with results of atomic calculations.[21]

As it is also evident from the XAS spectrum, the excitation probabilities and lifetimes of the individual intermediate states are rather different. Related differences will also be present for the autoionization decay probabilities of the intermediate $4d^9 4f^1$ states. Due to the substantial overlap of the $4d$ and $4f$ wave functions the singlet $^1P_1$ intermediate state reveals a large Auger transition rate for the participator decay leading to a $5p^5 4f^0$ final-state configuration. On the other hand, for a participator decay of the triplet states the direct transition ($4f \rightarrow 4d; 5p \rightarrow \epsilon l$; here ϵl denotes a state of the outgoing electron with energy ϵ and orbital momentum l) is spin-flip forbidden in LS coupling and is essentially suppressed in a weak intermediate coupling, while the exchange transition ($5p \rightarrow 4d; 4f \rightarrow \epsilon l$) has a low probability caused by relatively small overlap of the $4d$ and $5p$ wave functions. Thus, it may be expected that for the triplet intermediate states a spectator process involving valence $5d$ electrons ($5p \rightarrow 4d; 5d \rightarrow \epsilon l$ or $5d \rightarrow 4d; 5p \rightarrow \epsilon l$) could have a probability of the same order of magnitude as that of the participator process. Therefore, it should be taken into account for an accurate description of the line shape of resonant PE spectra. The spectator process results in a $5p^5 4f^1$ final-state configuration and may lead, therefore, to resonant enhancement of the $4f^1$ contribution in La $5p$ PE spectra.

An important role of the valence $5d$ electrons in the decay processes has already been assumed for the interpretation of the La $5p$ resonant PE spectra of LaB$_6$.[19] In this paper, however, solely a coincidence in energy positions of the $N_{4,5}O_{2,3}V$ Auger-like deexcitation of the $4d^9 4f^1$ intermediate state and the $5p$ PE signal upon excitation into the $^3D_1$ resonance has been concluded. In the present model of mixed final states both participator and spectator processes will contribute at all resonance energies to $|\phi^0\rangle$ and $|\phi^1\rangle$ according to the values of the coefficients c_{ij}. Note that the energy separation of the mixed $|\phi^0\rangle$ and $|\phi^1\rangle$ final states (2.1 eV) is close to the value of the spin-orbit splitting of the $5p$ core level (2.5 eV). Consequently, the $5p_{3/2}$ peak from the $|\phi^1\rangle$ final state will overlap in part the $5p_{1/2}$ peak related to the $|\phi^0\rangle$ final state. Spectral structures induced by spectator decays are expected to be broader than those originating from participator transitions, since in the former case in addition to the lifetime of the core hole, also the width of the occupied part of the $5d$ valence band has to be accounted for.

B. Theoretical model and details of calculations

The contributions of the individual final states to the spectral intensity of resonant PE may be summed up as

$$I(\epsilon,\omega) = \frac{2\pi}{\hbar} \sum_f |\langle f|T|g\rangle|^2 \delta(\hbar\omega + E_g - E_f), \qquad (3)$$

where $\hbar\omega$ is the incident photon energy, ϵ is the kinetic energy of the photoelectron, $|g\rangle$ is the ground state, and $|f\rangle$ is the final state of the system with the related energies E_g and E_f, respectively. Correspondence to the notations used before is established via the relations $|f\rangle = |\phi^i\rangle|\epsilon l\rangle$ and $E_f - E_g = W + \epsilon + \epsilon_B(\phi^i)$, where W denotes the work function and $\epsilon_B(\phi^i)$ the binding energy.

The transition matrix element can be expressed as[22]

$$\langle f|T|g\rangle = T(\epsilon) + \sum_r \left[\frac{V_r(\epsilon)}{\epsilon - \epsilon_r - i\Gamma_r} T_{0,r} \right.$$
$$\left. + \frac{V_r(\epsilon)}{\epsilon - \epsilon_r - i\Gamma_r} \int d\epsilon' \frac{V(\epsilon')T(\epsilon')}{\epsilon - \epsilon' - i\delta} \right], \qquad (4)$$

where the first term is the dipole matrix element describing the direct PE, the second term represents a dipole transition to the intermediate state r ($^3P_1$, $^3D_1$, and $^1P_1$ states in the case of the $4d \rightarrow 4f$ resonance in La) with the matrix element $T_{0,r}$ followed by Auger decay to the continuum with the matrix element $V_r(\epsilon)$. The energy dependences of $V_r(\epsilon)$ and $T(\epsilon)$ are weak and neglected in the restricted energy range considered, taking the value at the $^3D_1$ excitation. The Γ_r denote the inverse lifetimes. The third term describes a transition to a state off the energy shell $[T(\epsilon')]$ followed by a transition to the intermediate state $[V(\epsilon')]$ with a subsequent decay to the on-shell continuum and will be neglected in the following. Certainly, all matrix elements depend on the particular final state, but the corresponding indices are omitted in Eq. (4).

Dipole and Auger transition matrix elements have been evaluated using outgoing spherical waves and scalar-relativistic atomic wave functions calculated in the crystal potential. To this end, metallic La was simulated by a system of spherically symmetric potentials (overlapping atomic spheres), exploiting the Mattheiss construction.[23] For the exchange and correlation potential the von Barth–Hedin approximation[24] was used. In the case of the participator process the expressions for the calculations of the Auger transition rate in LS coupling for atoms with open shells were taken from Ref. 25, whereas for the spectator process the corresponding formulas have been derived from those given in Refs. 25 and 26 using Racah algebra. Relaxation of the intermediate state orbitals in the potential of the $4d$ hole was properly taken into account. The number of $5d$ electrons, $x = 2.2$, was taken from DFT ground-state calculations, using a linear-combination-of-atomic-orbitals population analysis. For the intermediate coupling calculation, we have used an expansion of the $^3P_1$, $^3D_1$, and $^1P_1$ states in terms of pure LS states taking the same values of Slater integrals and spin-orbit coupling constants as in Ref. 10. The only remaining free parameters in the intensity calculations were the inverse lifetimes, Γ_r, of the intermediate states that were estimated from the linewidths of the corresponding structures in the XAS spectrum.

C. Experimental results and discussion

Figure 2 presents on-resonance PE spectra taken at the $^3P_1$, $^3D_1$, and $^1P_1$ excitation thresholds (lines through experimental points) in comparison to off-resonance spectra

TABLE I. Auger transition amplitudes V_r and related branching ratios in La^{3+} for the participator decay of the intermediate states (considering intermediate coupling) into final states with outgoing d electron.

| Final | Intermediate state | | |
state	$^3P_1$	$^3D_1$	$^1P_1$
$5p_{1/2}^5 \epsilon d_{3/2}$	-0.0333	-0.0395	0.2745
$5p_{3/2}^5 \epsilon d_{3/2}$	-0.0554	-0.0063	0.1227
$5p_{3/2}^5 \epsilon d_{5/2}$	0.0194	-0.0084	0.3727
γ	0.32	14.21	0.49

(thick lines), measured below the respective resonant excitations. The $5p$ PE signal strongly resonates upon excitation into the $^1P_1$ intermediate state, its intensity increases by a factor of 6 in comparison to the off-resonance spectrum taken at 112 eV. The line shape of the on-resonance spectrum is nearly unchanged with respect to the off-resonance spectrum, and the intensity branching ratio $I(5p_{1/2})/I(5p_{3/2})$ is close to its statistical value of 1:2. In contrast, for the triplet intermediate states the $5p_{3/2}$ component reveals almost no intensity variations, whereas $5p_{1/2}$ component is considerably enhanced at both $^3P_1$ and $^3D_1$ resonances. Particularly, at the $^3D_1$ resonance this component becomes clearly dominating.

Assuming pure LS intermediate states, the branching ratio of participator Auger decay contributions, $\gamma = I_A(5p_{1/2})/I_A(5p_{3/2})$, can be obtained with the help of so-called jj-LS transformation coefficients.[27] In this way, the values $\gamma = 1:5$, 1:1, and 1:2 are found for the $^3P_1$, $^3D_1$, and $^1P_1$ intermediate states, respectively, and outgoing ϵd electrons. Thus, the intensity branching ratio of the $5p_{1/2}$ and $5p_{3/2}$ resonant PE peaks could show strong variations deviating from 1:2, if the contribution of the participator Auger decay to the resonant PE is comparable or higher than the contribution of direct PE. For outgoing ϵs electrons the respective values of γ are equal to 2:1 and 1:2 for the $^3P_1$ and $^1P_1$ states (the pure $^3D_1$ state cannot decay via this channel). In the present case, Auger processes creating an outgoing d electron dominate over Auger decays resulting in an outgoing s electron. The ratios of the related matrix elements lie between 2 and 12. It should be noted, that this situation is opposite to direct PE, where the dipole matrix element for transitions from the $5p$ level to continuum s states exceeds the matrix element for transitions to d states by one order of magnitude at the photon energies considered.

The intensity ratios given above are considerably changed if the intermediate states are not treated as pure LS states. As seen from Table I, for the triplet intermediate states the γ values calculated in intermediate coupling are increased in comparison to the ''pure'' values obtained from the jj-LS transformation. However, the branching ratio for the $^3P_1$ state is still about 1:3. Therefore, the participator channel alone cannot lead to the seeming enhancement of the $5p_{1/2}(\phi^0)$ component at this resonance (see Fig. 2). For the $^3D_1$ state the calculations give a strong increase of γ by a factor of 14. Even larger theoretical values (up to 36) were reported for the latter ratio in Refs. 10 and 20. These deviations can be explained by the low values of the participator

TABLE II. Contributions to the PE intensities in the energy region of the La $4d \rightarrow 4f$ excitation threshold. Values are given for final states without mixing. The intensities are normalized to the $5p_{3/2}$ direct PE intensity at the $^1P_1$ resonance. Note the energy shift ΔE of the spectator decay contributions.

Intermediate state	Direct PE		Tail of the giant res.		Participator decay to f^0 final state		Spectator decay to f^1 final state	
	$5p_{1/2}$	$5p_{3/2}$	$5p_{1/2}$	$5p_{3/2}$	$5p_{1/2}$	$5p_{3/2}$	$5p_{1/2}$	$5p_{3/2}$
$^3P_1$	0.94	1.88	0.45	0.91	0.16	0.39	0.15	0.30
$^3D_1$	0.88	1.76	0.69	1.38	0.85	0.07	0.47	0.93
$^1P_1$	0.50	1.00			26.29	53.70	0.15	0.30

Auger transition amplitudes involving the $5p_{3/2}$ states, which are extremely sensitive to rather small variations in the radial matrix elements (note that the values of the Auger transition amplitudes, presented in Table I, are consistent with those published in Ref. 10 in spite of different potentials and calculation procedures applied).

So far, we can state that consideration of the direct and participator channels may provide intensity branching ratios strongly deviating from 1:2, but cannot satisfactorily account for the experimentally observed values. To describe the PE spectra in Fig. 2 properly, we have to consider additional contributions to the resonant PE intensity. As can be seen from Table II, the probability of a spectator decay at the $^1P_1$ resonance is negligible as compared to that of a participator decay. For the triplet intermediate states, however, the spectator processes contribute considerably to the resonant PE intensity. Their contributions are of the same order of magnitude as those of the participator channels in accordance with the qualitative consideration in Sec. IV A. The effect of the indirect channels at the resonances can be estimated by comparison of the corresponding signals with direct PE intensities. At the $^1P_1$ giant resonance, the participator channel enhances the PE intensity by a factor of 50. Considering the effect of the extended tail of the $^1P_1$ resonance on the intensity of the off-resonance signal ($h\nu = 112$ eV), this factor is reduced to about 10 in fair agreement with the experiment (Fig. 2). For the understanding of the PE spectra taken at the preresonances, we refer to our finding that the $5p_{1/2}(\phi^0)$ and $5p_{3/2}(\phi^1)$ components overlap each other energetically. Due to this overlap the spectator Auger transitions contribute significantly to the enhancement in the region of the $5p_{1/2}(\phi^0)$ component in the PE spectrum taken at the $^3P_1$ and $^3D_1$ preresonances and are to a large part responsible for the anomalous peak intensity ratio $I(5p_{1/2})/I(5p_{3/2})$ observed here. A further modification of the spectral intensities is obtained by including final-state mixing.

The final results of our calculations are presented in Figs. 3 and 4. To simulate the shape of the resonant PE spectra, spectral lines were assumed to be Lorentzian with 1.5-eV FWHM, except for the spectator transitions, where a larger FWHM value of 2.3 eV accounts for the d band width. The comparison of Figs. 2 and 3 shows that the used theoretical model describes the experimental results rather well. Particularly, the relative intensities of the $5p_{1/2}$- and $5p_{3/2}$-derived components in the region of the preresonances (solid lines in Fig. 3) are reproduced. Moreover, the calculations reveal the structure (marked A in Fig. 3) seen as shoulders on the high-BE side of the resonant PE spectra and attributed to the $5p_{1/2}$ component of the mixed $|\phi^1\rangle$ final states. In the experiment this feature is mostly pronounced at the $^3D_1$ preresonance, where the contribution from the spectator decay
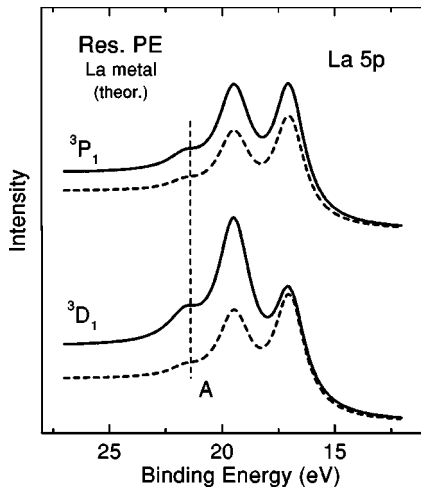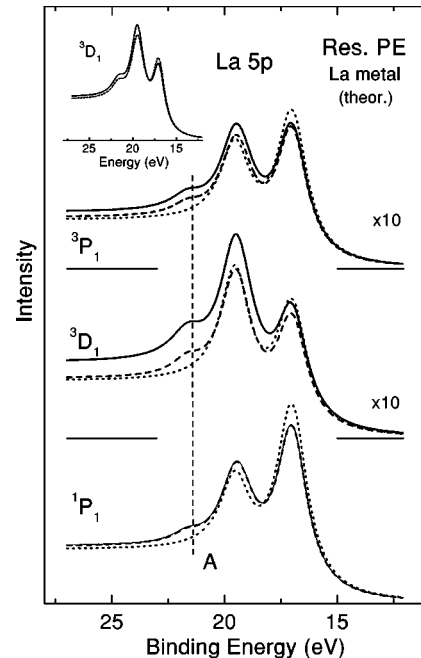

FIG. 4. Calculated on-resonance spectra at the $4d \rightarrow 4f$ excitation threshold (see text). Inset demonstrates the effect of coherent (solid line) and incoherent (dashed line) treatment of the direct and indirect channels in the case of the $^3D_1$ preresonance.

FIG. 3. Calculated on-resonance (solid lines) and off-resonance (dashed lines) spectra in the region of the $^3P_1$ and $^3D_1$ excitations.

channel is maximum. Note also the qualitative agreement between experiment and theory in the behavior of the $5p_{3/2}$-originating peak: at $^3P_1$ the on-resonance intensity is to some extent higher than the off-resonance intensity, at $^3D_1$ the on-resonance and off-resonance signals are almost equal. One can state even a quantitative consistency between the experimental and theoretical results in the region of the $^3D_1$ excitation. Some deviations of the calculated from the experimentally observed intensity ratios could be explained by a possible overestimation of Γ due to finite experimental resolution and neglect of hybridization effects in the ground and intermediate states.

The individual contributions of spectator channel and final-state mixing are disentangled in Fig. 4. As in Fig. 3, solid lines denote theoretical data, where all considered channels and final-state mixing are accounted for. Dashed lines represent related results where spectator channel contributions are excluded. Finally, dotted lines show the results with only direct PE and participator contributions included and final-state mixing neglected. For the $^1P_1$ spectrum, where the contribution of the spectator channel is negligible (see Table II), the effect of final-state mixing is essential to cause the observed shoulder A. Final-state mixing leads to a certain redistribution of spectral weight between $5p_{1/2}$ and $5p_{3/2}$ related features. For the $^3D_1$ spectrum the effect of spectator transitions exceeds that of the final-state mixing, whereas for the $^3P_1$ spectrum the roles of both events in the formation of the line shape are approximately equal.

An important issue to be clarified for the theoretical treatment is that of coherence of the direct and indirect processes in resonant PE, i.e., the question as to whether amplitudes or intensities should be summed up to describe the resonant PE spectrum. It was demonstrated in Ref. 12 that not only energy overlap, but also temporal matching is required for true ''resonant PE.'' For the $4d \rightarrow 4f$ resonance in Gd, the super-Coster-Kronig autoionization of the intermediate state is almost coherent to the direct $4f$ PE. In the case of the Gd $5p$ core level, however, the authors conclude that the coherency is lost because the indirect Coster-Kronig process is about six times slower than the super-Coster-Kronig transition. The $4d^9 4f^1$ intermediate state in La excludes the super-Coster-Kronig decay channel. Here, the participator decay is a Coster-Kronig transition at the giant resonance $^1P_1$. The par-

ticipator decays of the triplet $^3P_1$ and $^3D_1$ states, where the Coster-Kronig transition is spin-flip forbidden in LS coupling (see above), as well as the spectator decay processes are even slower than the decay of the $^1P_1$ state. From this point of view, all indirect channels are expected to be incoherent with direct PE. For the theoretical results presented above, a coherent superposition of all considered channels was used. By comparison with an incoherent treatment of direct and indirect channels, we have found, however, that the influence of the interference terms is not decisive (see inset in Fig. 4). The reason is that different decay channels contribute mostly to nonequivalent $|\epsilon l\rangle$ states of the outgoing electron ($l=0$ for direct PE, $l=2$ for participator process, $l=1,3$ for spectator process).

V. CONCLUSIONS

We have shown that the La $5p$ PE spectra consist of a superposition of two mixed final states, based on $5p^5 4f^0$ and $5p^5 4f^1$ configurations. They reveal different resonant enhancements across the $4d \rightarrow 4f$ excitation threshold. In contrast to the case of Sm or Eu, where a different resonant behavior of divalent and trivalent ions is related to nonequivalent $4f$ occupancies in the intermediate state,[5] in La metal the phenomenon is caused by the interplay between spectator and participator decay processes with the final-state mixing.

Our understanding of the selective resonant enhancements of different final-state configurations based on the experimental data taken for the model case of the La $5p$ states can be extended to more complicated systems. Similar effects are expected to be relevant for the resonant behavior of other light RE's and may be responsible for the satellite structures observed in the resonant PE spectra of several Pr and Nd compounds.[28] Analogous phenomena are expected for actinide and transition-metal systems.

ACKNOWLEDGMENTS

---

*On leave from Institute of Physics, St. Petersburg State University, 198904 St. Petersburg, Russia.

†On leave from Dto. de Fisica de la Materia Cond., Universidad Autonoma de Madrid, E-28049 Madrid, Spain.

[1] For a review see J.W. Allen, in *Synchrotron Radiation Research—Surface and Interface Science*, edited by R. Z. Bachrach (Plenum Press, New York, 1992), Vol. 1, p. 253.

[2] C. Guillot, Y. Ballu, J. Paigne, J. Lecante, K. P. Jain, P. Thiry, R. Pinchaux, Y. Petroff, and L. M. Falicov, Phys. Rev. Lett. **39**, 1632 (1977); R. Clanberg, W. Gudat, E. Kisker, E. Kuhlmann, and G. M. Rothberg, *ibid.* **47**, 1314 (1981); L. H. Tjeng, C. T. Chen, J. Ghijsen, P. Rudolf, and F. Sette, *ibid.* **67**, 501 (1991).

[3] W. Lenth, F. Lutz, J. Barth, G. Kalkoffen, and C. Kunz, Phys. Rev. Lett. **41**, 1185 (1978); J. W. Allen, L. I. Johansson, R. S. Bauer, I. Lindau, and S. B. M. Hagstrom, *ibid.* **41**, 1499 (1978); W. F. Egelhoff, Jr., G. G. Tibbetts, M. H. Hecht, and I. Lindau,

ibid. **46**, 1071 (1981).

[4] F. Gerken, J. Barth, and C. Kunz, Phys. Rev. Lett. **47**, 993 (1981).

[5] W. D. Schneider, C. Laubschat, G. Kalkowski, J. Haase, and A. Puschmann, Phys. Rev. B **28**, 2017 (1983).

[6] C. Laubschat, E. Weschke, G. Kalkowski, and G. Kaindl, Phys. Scr. **41**, 124 (1990).

[7] E. Weschke, C. Laubschat, T. Simmons, M. Domke, O. Strebel, and G. Kaindl, Phys. Rev. B **44**, 8304 (1991).

[8] M. Iwan, E. E. Koch, and F.-J. Himpsel, Phys. Rev. B **24**, 613 (1981); B. Reihl, M. Domke, G. Kaindl, G. Kalkowski, C. Laubschat, F. Hulliger, and W. D. Schneider, *ibid.* **32**, 3530 (1985); S. L. Molodtsov, J. Boysen, M. Richter, P. Segovia, C. Laubschat, S. A. Gorovikov, A. M. Ionov, G. V. Prudnikova, and V. K. Adamchuk, *ibid.* **57**, 13 241 (1998).

[9] C. G. Olson, P. J. Benning, M. Schmidt, D. W. Lynch, P. Canfield, and D. M. Wieliczka, Phys. Rev. Lett. **76**, 4265 (1996); S.

L. Molodtsov, M. Richter, S. Danzenbächer, S. Wieling, L. Steinbeck, and C. Laubschat, *ibid.* **78**, 142 (1997).

[10] H. Ogasawara, A. Kotani, B. T. Thole, K. Ishikawa, O. Aita, and M. Kamada, Solid State Commun. **81**, 645 (1992).

[11] C. L. Nicklin, C. Binns, S. Mozley, C. Norris, E. Alleno, M. G. Barthes-Labrousse, and G. van der Laan, Phys. Rev. B **52**, 4815 (1995).

[12] S. R. Mishra, T. R. Cummins, G. D. Waddill, W. J. Gammon, G. van der Laan, K. W. Goodman, and J. G. Tobin, Phys. Rev. Lett. **81**, 1306 (1998).

[13] J. K. Lang, Y. Baer, and P. A. Cox, J. Phys. F: Met. Phys. **11**, 121 (1981); A. V. Fedorov, C. Laubschat, K. Starke, E. Weschke, K.-U. Barholz, and G. Kaindl, Phys. Rev. Lett. **70**, 1719 (1993).

[14] J.-M. Esteva, R. C. Karnatak, J. C. Fuggle, and G. A. Sawatzky, Phys. Rev. Lett. **50**, 910 (1983).

[15] O. Gunnarsson and K. Schönhammer, Phys. Rev. Lett. **41**, 1608 (1978); Phys. Rev. B **31**, 4815 (1985).

[16] J.-M. Imer and E. Wuilloud, Z. Phys. B: Condens. Matter **66**, 153 (1987).

[17] The effective Coulomb interaction between $4f$ electron and core hole, U_{fc}, has been estimated by calculating the shift of the atomic $4f$-$5d$ promotion energy, $E_{f\text{-}d}^{at}$, upon introduction of the respective core hole: $U_{fc} \approx E_{f\text{-}d}^{at}[c^n] - E_{f\text{-}d}^{at}[c^{n-1}]$, where $E_{f\text{-}d}^{at} = E^{at}[f^0 d^1 s^2] - E^{at}[f^1 d^0 s^2]$. The energies of the related configurations were obtained from fully relativistic, self-interaction corrected, local spin density approximation atomic total energy calculations [J. Forstreuter, L. Steinbeck, M. Richter, and H. Eschrig, Phys. Rev. B **55**, 9415 (1997); H. Eschrig and V. D. P. Servedio, J. Comput. Chem. **20**, 23 (1999)].

[18] E. Weschke, A. Höhr, G. Kaindl, S. L. Molodtsov, S. Dauzenbächer, M. Richter, and C. Laubschat, Phys. Rev. B **58**, 3682 (1998).

[19] M. Aono, T.-C. Chiang, J. A. Knapp, T. Tanaka, and D. E. Eastman, Phys. Rev. B **21**, 2661 (1980).

[20] C. Bonnelle, G. Giorgi, and J. Bruneau, Phys. Rev. B **50**, 16 255 (1994).

[21] Consideration of hybridization effects in the ground (f occupancy 0.017) and intermediate states would lead to the appearance of new $4d^9 4f^m$ intermediate states with different $4f$ occupancy m. A quantitative treatment of this effect is complicated due to the strong $4d$-$4f$ interactions that cause broad and overlapping $4d^9 4f^0$ and $4d^9 4f^1$ multiplets [see Y. Baer and W.-D. Schneider, in *Handbook of the Physics and Chemistry of Rare Earths*, edited by K. A. Gschneider, Jr., L. Eyring, and S. Hüfner (North-Holland, Amsterdam, 1987), Vol. 10, p. 30]. These effects, however, are obviously weak, since no contributions of $4d^9 4f^0$ and $4d^9 4f^2$ states are obtained in the XAS spectrum of La metal (see inset in Fig. 2).

[22] C.-O. Almbladh and L. Hedin, in *Handbook on Synchrotron Radiation*, edited by E. E. Koch (North-Holland, Amsterdam, 1983), Vol. 1b, p. 607.

[23] L. F. Mattheiss, Phys. Rev. **133**, A1399 (1964); **134**, A970 (1964).

[24] U. von Barth and L. Hedin, J. Phys. C **5**, 1629 (1972).

[25] E. McGuire, Phys. Rev. A **12**, 330 (1975).

[26] E. McGuire, Phys. Rev. A **10**, 32 (1974).

[27] D. A. Varshalovich, A. N. Moskalev, and V. K. Khersonskii, *Quantum Theory of Angular Momentum* (World Scientific Publishing, Singapore, 1988).

[28] R. D. Parks, S. Raaen, M. L. Denboer, Y.-S. Chang, and G. P. Williams, Phys. Rev. Lett. **52**, 2176 (1984); G. Kalkowski, E. V. Sampathkumaran, C. Laubschat, M. Domke, and G. Kaindl, Solid State Commun. **55**, 977 (1985).